Theoretical Study of Photophysical Properties of Bisindolylmaleimide Derivatives

Kenichiro Saita,[‖,†,‡] **Manabu Nakazono,**[§] **Kiyoshi Zaitsu,**[§] **Shinkoh Nanbu,**[‖,*,‡] **and Hiroshi Sekiya***[,†]

Department of Chemistry, Faculty of Science, Graduate School of Molecular Chemistry, Kyushu University, 6-10-1 Hakozaki, Higashi-ku, Fukuoka 812-8581, Japan, Research Institute for Information Technology, Kyushu University, 6-10-1 Hakozaki, Higashi-ku, Fukuoka 812-8581, Japan, and Graduate School of Pharmaceutical Sciences, Kyushu University, 3-1-1 Maidashi, Higashi-ku, Fukuoka 812-8582, Japan

Received: May 10, 2009; Revised Manuscript Received: June 9, 2009

The photophysical properties of two bisindolylmaleimide derivatives, 3,4-bis(3-indolyl)-1-*H*-pyrrole-2,5-dione (arcyriarubin A) and indolo[2,3-a]pyrrolo[3,4-c] carbazole-5,7-(6 *H*)-dione (arcyriaflavin A), are investigated by using ab initio molecular orbital (MO) and multireference perturbation theory. These compounds are suggested to exist as monovalent anions deprotonated from an indole NH group in aprotic polar solvents. The analysis of MOs shows that the electronic structures of the S_1 and S_2 states are described by the single- or double-electron excitation between the naturally localized MOs on an indole moiety and on the maleimide part. This indicates that the intramolecular charge transfer (ICT) transfer may occur by photoexcitation. The minimum-energy structure of the arcyriarubin A anion is twisted; the dihedral angles between the indole and maleimide rings are 83.4° and 20.2° for the S_1 and S_0 states, respectively. The analysis of the minimum energy path along the coordinate of the twist angle is performed to explore the emission process from the S_1 state. It has been shown that the magnitude of the Stokes shift increases with increasing the twist angle, but the oscillator strength decreases. It has been suggested that the experimentally observed fluorescence arises on the way toward the energy minimum of the S_1 state. The Stokes-shifted emission of arcyriaflavin A is contributed by the S_1−S_0 electronic relaxation after the excitation in the S_2 state.

Introduction

Bisindolylmaleimide derivatives such as arcyriarubin and arcyriaflavin, which are isolated from the fruiting bodies of the slime mold (*Arcyria denudata*),[1] contain both two indole subunits and a maleimide subunit. These compounds correspond to a core structure of selective inhibitors of protein kinase C (PKC) or DNA topoisomerase, as staurosporine,[2] rebeccamycin,[3] and ICP-1,[4] which have a bisindolylmaleimide or indolocarbazole skeleton with a C−N linkage to a sugar moiety. The ability of selective inhibition or regulation of the metabolism of cells makes them therapeutically important anticancer agents.[5] The PKC isoenzyme family members phosphorylate a wide variety of protein targets, and they are involved in diverse cellular signaling or signal transduction.[6] Consequently the PKC inhibitors such as these bisindolylmaleimide derivatives are promising therapy agents for autoimmune diseases and tumors.[4,7]

On another matter, fluorescent, chemiluminescent, and bioluminescent compounds have been developed for luminescence assays,[8−10] especially for specific detection of certain biomolecules.[11−13] Various indole derivatives were also synthesized, and their luminescent characteristics were investigated.[14,15] A number of bisindolylmaleimide derivatives exhibit strong fluorescence accompanying a large Stokes shift with respect to the absorption wavelength, which leads to suitable luminescence assays available for a specific detection.[16,17] Most bisindolylmaleimides are vivid red crystals[1] and some of them exhibit red luminescence in their solid phase; amorphous films of *N*-methylated derivatives have been applied for fabrication of red light-emitting diodes (LEDs).[18]

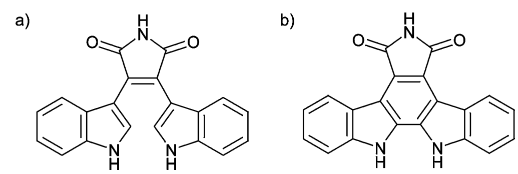

Figure 1. Molecular structures of **BIM** and **C-BIM**.

The origin of the large Stokes shift of the emission of bisindolylmaleimides in solution has not been fully understood. In general, it is caused by a significant difference between the equilibrium geometry of the lowest electronic excited state and that of the electronic ground state,[19−22] but a large Stokes-shift may also occur due to the energy relaxation from higher excited states to the lowest excited state.[23] It is considered that the intramolecular charge transfer (ICT) is responsible for the phenomenon. ICT appears in the electronic ground and/or electronically excited states of the indolylmaleimide derivatives, because these molecules have the well-known electron donor−acceptor feature provided by the indole and maleimide groups. Kaletas et al. investigated the solvatochromic behavior to verify whether the ICT character dominates the spectroscopic properties of arcyriarubin A (*N*-H bisindolylmaleimide, **BIM**) and arcyriaflavin A (cyclized *N*-H bisindolylmaleimide, **C-BIM**).[17] The molecular structures of **BIM** and **C-BIM** are displayed in Figure 1. According to the Kamlet−Taft treatment,[24] the observed emission spectra show slightly solvatochromic trends.

* To whom correspondence should be addressed. E-mail: sekiya@chem.kyushu-univ.jp (H.S.); shinkoh.nanbu@sophia.ac.jp (S.N.).
† Graduate School of Molecular Chemistry.
‡ Research Institute for Information Technology.
§ Graduate School of Pharmaceutical Sciences.
‖ Present address: Department of Materials and Life Sciences, Faculty of Science and Technology, Sophia University, 7-1 Kioi-cho, Chiyoda-ku, Tokyo 102-8554, Japan.

10.1021/jp9043489 CCC: $40.75

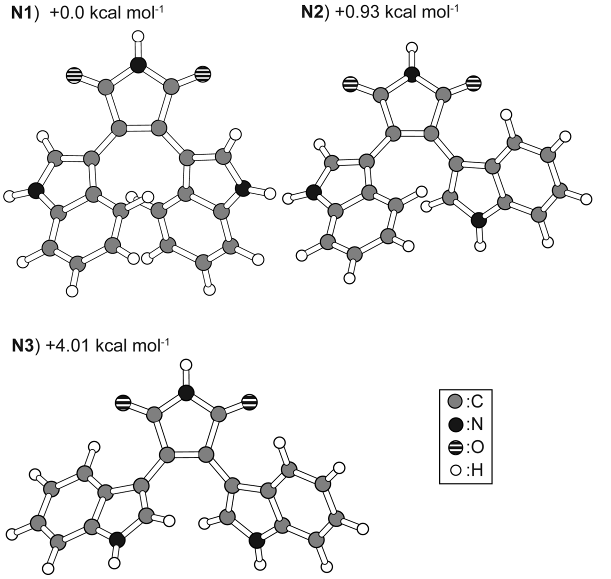

Figure 2. Optimized structures of neutral **BIM** obtained by CASPT2/cc-pVDZ calculations and their relative potential energies are indicated in units of kcal mol^{-1}.

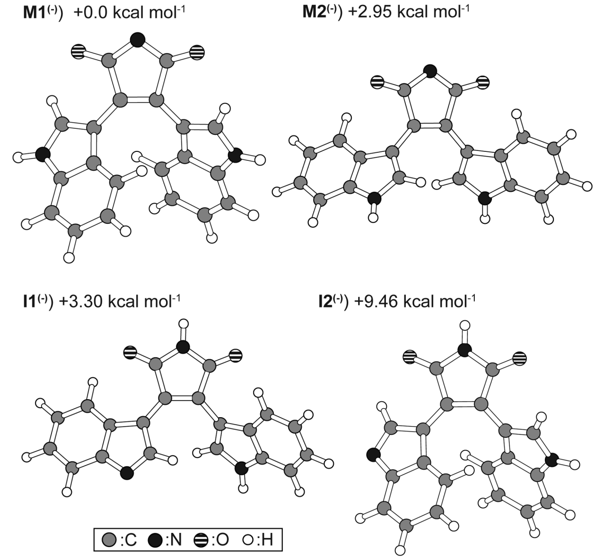

Figure 3. Optimized structures of deprotonated anions (**M1**$^{(-)}$, **M2**$^{(-)}$, **I1**$^{(-)}$, and **I2**$^{(-)}$) of **BIM** obtained by CASPT2/cc-pVDZ calculations and their relative potential energies are indicated in units of kcal mol^{-1}.

TABLE 1: Potential Energies of the S_0, S_1, and S_2 States and the Oscillator Strengths and the Excitation Energies for the Electronic Transitions of the Three Isomers of Neutral BIM[b]

	electronic state	E/cm^{-1}	oscillator strength	λ/nm our theo.	λ/nm exp[a]
N1	S_0	0			
	S_1	30508	0.32	327	366
	S_2	37317	0.14	268	
N2	S_0	0 (325)			
	S_1	30574 (30899)	0.28	327	
	S_2	36548 (36873)	0.16	274	
N3	S_0	0 (1254)			
	S_1	28949 (30245)	0.18	345	
	S_2	37456 (38712)	0.12	267	

[a] Figures in parentheses in the column of E(energy)/cm^{-1} stand for the relative energy to the S_0 state of the most stable isomer. [b] Reference 16.

TABLE 2: Potential Energies of the S_0, S_1, and S_2 States and the Oscillator Strengths and the Excitation Energies for the Electronic Transitions of the Four Isomers of Deprotonated Anion of BIM[a]

	electronic state	E/cm^{-1}	oscillator strength	λ/nm our theo.	λ/nm exp[b]
M1$^{(-)}$	S_0	0			
	S_1	30835	<0.01	324	
	S_2	35146	<0.01	284	
M2$^{(-)}$	S_0	0 (1030)			
	S_1	30375 (31405)	<0.01	329	
	S_2	34042 (35072)	<0.01	294	
I1$^{(-)}$	S_0	0 (1156)			
	S_1	22231 (23387)	0.42	450	452
	S_2	30590 (31746)	0.05	327	(366)
I2$^{(-)}$	S_0	0 (3307)			
	S_1	24592 (27899)	0.52	406	
	S_2	31348 (34655)	<0.01	319	

[a] Two of the four are the deprotonated form of the maleimide NH group (**M1**$^{(-)}$ and **M2**$^{(-)}$), and the other are the deprotonated form of the indole NH group (**I1**$^{(-)}$ and **I2**$^{(-)}$). Figures in parentheses in the column of E (energy) /cm^{-1} stand for the relative energy to the S_0 state of the most stable isomer. [b] Reference 16.

However their quantum chemical calculations with density functional theory (DFT) indicate that all of the orbitals, which are involved in the electronic transitions exhibit a delocalization of the electron density over the whole molecule, therefore, we cannot expect ICT in which the electron density transferred from one indole unit to the maleimide part. They finally concluded that no ICT occurs in **BIM** and **C-BIM**. On the other hand, immediately after the report of Kaletas et al., Kosower and de Souza pointed out that the slopes of the plots of emission energies against $E_T(30)$ for these bisindolylmaleimide derivatives, **BIM** (0.37) and **C-BIM** (0.54), would establish that the emissions arise from the charge transfer.[25] Thus, it is still a subject of controversy whether ICT does occur in **BIM** and **C-BIM** or not. Furthermore, the DFT calculation is suitable to explore the features of the electronic ground state around the equilibrium geometry, whereas it could not be enough to describe the electronic structures related to the electronically excited states, especially in the donor−acceptor type of the electronic state. At least two configuration state functions (CSFs) are required for the ab initio calculation of the present molecular system. In order to look into the possibility of the donor−acceptor type transition, the multiconfiguration self-consistent field (MCSCF) calculations with the complete active space (CAS) is employed to determine the molecular orbitals (MOs), and then the multireference perturbation calculation is performed with CSFs obtained by the MOs.

In this paper we investigate the photophysical properties of **BIM** and **C-BIM** on the grounds of our results of quantum chemistry calculations. The molecular structures at the potential minima and the potential energies for the electronic ground (S_0) state, the lowest electronic excited (S_1) state, and the second excited (S_2) state of these conformers (isomers) were obtained using the multireference perturbation theory along with use of CASSCF calculations. Details of these calculations are described in the method section. In the results and discussion section, we discuss the properties with our findings from **BIM** and those of **C-BIM** separately. In order to assign the species that are responsible for the absorption in an aprotic polar solvent, *N*,*N*-dimethylformamide (DMF), the vertical excitation energies and the transition dipole moments of the isomers are compared with

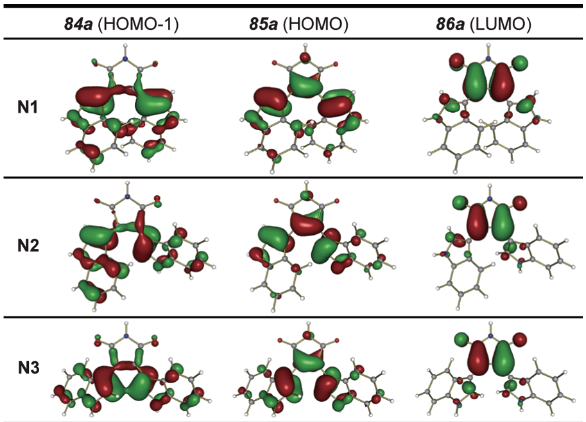

Figure 4. Molecular orbitals of isomers (**N1**, **N2**, and **N3**) of neutral BIM: (HOMO-1), HOMO, and LUMO.

the spectroscopic data.[16,17] Detailed discussions of the characters of the low-lying electronic states and the occurrence of the ICT are made on the basis of the results of the multireference perturbation calculation. We also discuss in this section the origin of the Stokes-shifted fluorescence of these bisindolylmaleimides. Finally we summarize and compare the results of **BIM** and **C-BIM** in the conclusion section.

Computational Methods

Our previous paper suggested that **BIM** and **C-BIM** exist as the monovalent or divalent anions in aprotic polar solvents such as DMF (*N*,*N*-dimethylformamide) on the grounds of the comparison between absorption maxima and vertical excitation energies calculated with the MRCI (multireference configuration interaction) method by using the optimized geometries at the B3LYP/cc-pVDZ level of theory.[16] However, we still have a doubt whether the most stable structure can be optimized by the single electronic configuration method based on DFT; the optimized structures we have reported might be misleading because the natural orbitals were not employed for the geometry optimization, especially for the charge-transfer system. In addition, only one anionic species which was deprotonated from the indole NH group has been theoretically explored in the previous paper, although the hydrogen atom of the maleimide NH group could be detachable.[17,26] We should take into account two monovalent anions, a deprotonated form of the NH group of the maleimide moiety and a deprotonated form of the NH group of one of the indole moieties, for each derivative since the two indole subunits were equivalent. Therefore, we again carried out geometry optimization of electronic neutral species of **BIM**, **C-BIM**, and their monovalent anions with the more reliable CASPT2 method,[27] because the MRCI method used in the previous paper was time-consuming for the system consisting of 25 heavy atoms and 13 (**BIM**) or 12 (**C-BIM**) hydrogen atoms to accomplish fully geometry optimizations. We employed Dunning's cc-pVDZ (correlation consistent, polarized valence, double-ζ) basis set.[28] In each step of the molecular geometry optimization, we first performed three-state-averaged complete active space self-consistent field (CASSCF) calculations[29] to determine the molecular orbital set for subsequent multireference perturbation calculations. Then the potential energy and the analytical gradient for the molecular geometry were obtained from the multireference perturbation calculations using second-order Rayleigh–Schrödinger perturbation theory (RS2).[27] The active spaces were employed as CAS(8,6) and CAS(6,5) for **BIM** and **C-BIM**, respectively. The main electronic configurations of the ground state of **BIM** (C_1 symmetry) and **C-BIM** (C_s symmetry) are written as

BIM (1^1A (S_0)): (inner occupied orbitals)^{162}(82a)^2(83a)^2(84a)^2(85a)^2(86a)^0(87a)^0,

C-BIM (1^1A′ (S_0)): (inner occupied orbitals)^{162}(82a″)^2(83a″)^2(84a″)^2(85a″)^0(86a″)^0.

The characters of each MO are mentioned in the later section. The canonical orbitals were obtained by the CASSCF calcula-

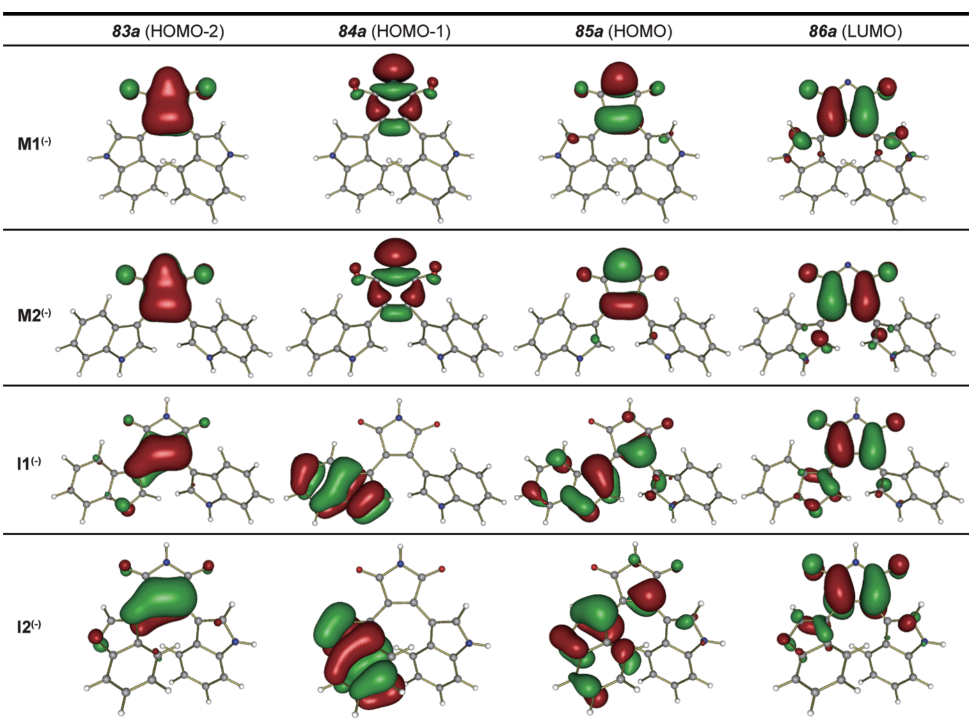

Figure 5. Molecular orbitals of isomers (**M1**$^{(-)}$, **M2**$^{(-)}$, **I1**$^{(-)}$, and **I2**$^{(-)}$) of deprotonated **BIM** anions: HOMO-2, HOMO-1, HOMO, and LUMO.

tion, and the configuration state functions (CSFs) were generated by single and double electron excitations based on the reference configurations obtained from the CASSCF calculations. In this work, the CSFs were generated with:

BIM: $[(82a)(83a)(84a)(85a)(86a)(87a)]^8$,

C-BIM: $[(82a'')(83a'')(84a'')(85a'')(86a'')]^6$.

The total number of configurations for multireference perturbation calculations with RS2 (CASPT2) of **BIM** was about 24 000 000, and that of **C-BIM** was about 19 000 000.

All of these quantum chemistry calculations were performed using the electronic structure program MOLPRO (revision 2006.1).[30] The computers on which calculations were performed were PRIMEQUEST 580 and PRIMERGY RX200S3 (Fujitsu) and SR11000 (Hitachi) owned by the computer center of Kyushu University.

Results and Discussion

I. Bisindolylmaleimide (BIM)/Arcyriarubin A.

i. Identification of Conformer in N,N-Dimethylformamide (DMF) Solution. Three stable conformers (**N1**-**N3**) of neutral **BIM** have been obtained by the geometry optimization for the S_0 state. These optimized structures are displayed in Figure 2 together with the relative potential energies. The relative energies are 0.0, 0.93, and 4.01 kcal mol^{-1} for **N1**, **N2**, and **N3**, respectively. The geometry optimization calculations have been performed in vacuo. The molecule in solution would walk up and down around these energy minima of these conformers.

The potential energies of the S_0, S_1, and S_2 states and the vertical excitation energies (S_1-S_0, S_2-S_0) for conformer **N1**−**N3** are listed in Table 1. The vertical excitation energies of all the conformers of neutral **BIM** are inconsistent with the low energy absorption band (λ_{max} = 452 nm).[16]

On the other hand, four stable conformers were found for anionic **BIM** in the electronic ground state; two stable conformers, **M1**$^{(-)}$ and **M2**$^{(-)}$ are the deprotonated form of the maleimide NH group, while the other two conformers, **I1**$^{(-)}$ and **I2**$^{(-)}$ are that of the indole NH group. The electronic ground states of deprotonated anions are also denoted as S_0. The structures of these isomers are displayed in Figure 3 and the potential energies of the S_0, S_1, and S_2 states and the vertical excitation energies (S_1-S_0, S_2-S_0) are listed in Table 2. It is particularly worth noting that the potential energies of the electronic excited states of **I1**$^{(-)}$ and **I2**$^{(-)}$ are lowered remarkably, whereas those of **M1**$^{(-)}$ and **M2**$^{(-)}$ are similar to the neutral species. The S_1-S_0 vertical excitation energy of isomer **I1**$^{(-)}$ is in good agreement with the absorbed energy (λ_{max} = 452 nm); furthermore, in terms of the calculated oscillator strength (f_0), the electronic transitions of **M1**$^{(-)}$ and **M2**$^{(-)}$ are almost forbidden ($f_0 < 0.01$), although the S_1-S_0 transitions of **I1**$^{(-)}$ and **I2**$^{(-)}$ are allowed. Hence, it is suggested that the **BIM** molecule exists as the **I1**$^{(-)}$ form in DMF solution. The relative energies of the S_0 state of **M1**$^{(-)}$, **M2**$^{(-)}$, **I1**$^{(-)}$, and **I2**$^{(-)}$ are 0.0, 2.95, 3.30, and 9.46 kcal mol^{-1}, respectively. It is interesting to note that the isomers, which are deprotonated from the maleimide NH group, are energetically more stable than the isomers deprotonated from an indole group. In vacuo, it is suggested that the deprotonation from the maleimide unit could occur more easily than that from an indole unit, because in the neutral isomers (**N1**−**N3**), the Coulombic attracting force between the N and H atoms of the indole units is stronger than that of the maleimide unit from viewpoints of the N−H bond lengths and of Mulliken population analysis. Generally speaking, however, the subtraction of hydrogen atoms from solute by the solvent may cause the deprotonation of nonacidic compounds in solution. Such an interaction between neutral **BIM** molecules and solvents is necessary to generate the **BIM** anions. In the previous paper, we have attempted the geometry optimization of the **BIM** and DMF (*N*,*N*-dimethylformamide) complexes, and finally obtained only one configuration having a hydrogen bond between the H atom of indole NH and the O=C group of the DMF molecule (see also the Supporting Information of ref 16). The subtraction of an H atom from an NH group of the indole moiety would occur more easily than from the maleimide NH in DMF solution. Thus, the major species in DMF solution is assigned as **I1**$^{(-)}$.

ii. MOs and Electronic Configurations of Isomers in Franck−Condon Region. The main electronic configuration of the ground state of **BIM** in CASPT2 is described as

$(1^1A\ (S_0))$: (inner occupied orbitals)$^{162}(82a)^2(83a)^2(84a)^2(85a)^2(86a)^0(87a)^0$.

However, there are additional contributions from electronic excitations such as

(inner occupied orbitals)$^{162}(82a)^2(83a)^1(84a)^2(85a)^1(86a)^2(87a)^0$,

(inner occupied orbitals)$^{162}(82a)^2(83a)^2(84a)^2(85a)^0(86a)^2(87a)^0$, and

(inner occupied orbitals)$^{162}(82a)^2(83a)^0(84a)^2(85a)^2(86a)^2(87a)^0$.

The molecular orbitals (MOs) are characterized by 83a (highest occupied molecular orbital, HOMO-2), 84a (HOMO-1), 85a (HOMO), and 86a (lowest occupied molecular orbital, LUMO) under C_1 symmetry. At least four MOs should be included in the active space. Finally, the six active orbitals are important to describe the low-lying electronic states, and these orbitals are occupied by eight electrons in CASSCF (8 electrons/6 MOs).

The primary configuration for the S_1 state of neutral **BIM** (**N1**-**N3**) is the single electron excitations to LUMO from HOMO which is indicated as $(\mathrm{HOMO})^1 \rightarrow (\mathrm{LUMO})^1$ and that of the S_2 state is $(\mathrm{HOMO\text{-}1})^1 \rightarrow (\mathrm{LUMO})^1$. Figure 4 illustrates these MOs, (HOMO-1), HOMO, and LUMO of **N1**-**N3**. The vertical excitation energies of all the conformers of neutral **BIM** are inconsistent with a low energy absorption band (λ_{max} = 452 nm[16]), and all of the electronic transitions could not be ascribed to the ICT process since the corresponding MOs are delocalized over the center of the molecule.

The primary electronic configuration of the S_0 state of anionic BIM (**M1**$^{(-)}$, **M2**$^{(-)}$, **I1**$^{(-)}$, and **I2**$^{(-)}$) is also described as

$(1^1A\ (S_0))$: (inner occupied orbitals)$^{162}(82a)^2(83a)^2(84a)^2(85a)^2(86a)^0(87a)^0$, since the isomers are deprotonated anions. The other electronic configurations which contribute to the electronic ground and excited states are listed in Table 2. Figure 5 illustrates their MOs, (HOMO-2), (HOMO-1), HOMO, and LUMO of these isomers, which are determined by our MCSCF calculations. For all these isomers, a main character of the S_1 state corresponds to a single electron excitation of $(\mathrm{HOMO})^1 \rightarrow (\mathrm{LUMO})^1$, and that of the S_2 state corresponds to $(\mathrm{HOMO\text{-}1})^1 \rightarrow (\mathrm{LUMO})^1$. The difference between **M1**$^{(-)}$, **M2**$^{(-)}$, **I1**$^{(-)}$, and **I2**$^{(-)}$ is seen in the secondary or the tertiary electronic configurations (the configurations are listed in Table S2 of the Supporting Information). It is clearly seen that these excitation, HOMO−LUMO, or (HOMO-1)−LUMO, of isomer **I1**$^{(-)}$ corresponds to the electron transfer from π-MO localized on the deprotonated indole moiety to π*-MO localized on the maleimide moiety, i.e. this electronic transition corresponds to the ICT process. Although the single electron excitation to an antibonding π*-MO causes destabilization of the molecule, it is suggested that the charge−charge interaction stabilizes the excited states. On the other hand, HOMO−LUMO or (HOMO-

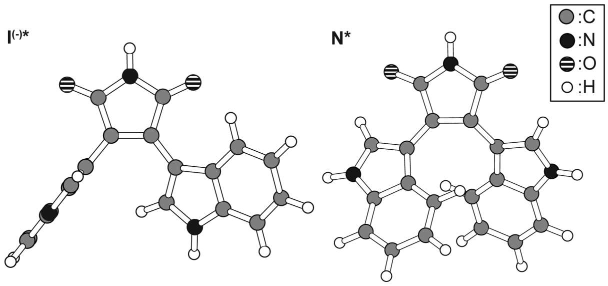

Figure 6. Optimized structure in the S_1 state of the monovalent anions of **BIM** ($\mathbf{I}^{(-)}$*) and that of the neutral **BIM** (**N***).

TABLE 3: Potential Energies of the S_0 and S_1 States and the Oscillator Strengths and the Value of Stokes Shift of the S_0-S_1 Electronic Transition for the Optimized Structure in the S_1 State of Monovalent Anions of BIM ($\mathbf{I}^{(-)}$*)

	electronic state	E/cm^{-1}	oscillator strength	Stokes shift/cm^{-1}
$\mathbf{I}^{(-)}$*	S_0	0		
	S_1	9296	0.002	12935
exp[a]		16667		5457

[a] Reference 16.

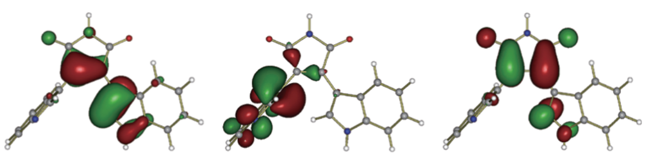

84a (HOMO-1) *85a* (HOMO) *86a* (LUMO)

Figure 7. (HOMO-1), HOMO, and LUMO of $\mathbf{I}^{(-)}$*.

1)−(LUMO) excitation of $\mathbf{M1}^{(-)}$ and $\mathbf{M2}^{(-)}$ corresponds to the $\pi-\pi^*$ transition localized on the maleimide moiety. In the other words, the ICT process is not involved in the electronic transition of $\mathbf{M1}^{(-)}$ and $\mathbf{M2}^{(-)}$.

iii. Optimized Structure of S_1 and Origin of Stokes Shift. In order to investigate the origin of the large Stokes shift of the **BIM** molecule in solution,[16,17] we have carried out the molecular geometry optimization to search the energy minimum in the S_1 potential surface of the monovalent anion, which is deprotonated from an indole NH group assigned above to the species existing in solution. The optimized structure in the S_1 state of monovalent anions of **BIM** denoted by $\mathbf{I}^{(-)}$* is displayed in Figure 6, while the potential energies and the vertical transition energies to the S_0 corresponding to theoretical emission energies are listed in Table 3. The optimized geometry of $\mathbf{I}^{(-)}$* changes dramatically. The deprotonated indole subunit in $\mathbf{I}^{(-)}$* is twisted, and it makes a dihedral angle of 83.4° with the maleimide unit, which is close to a right angle. The potential energy at the optimized geometry in the S_1 state of $\mathbf{I}^{(-)}$* prominently decreased by 5920 cm^{-1} from the energy of the Franck−Condon (FC) region in the potential surface of $\mathbf{I1}^{(-)}$. The HOMO−LUMO single excitation is the primary configuration even for the optimized geometry in the S_1 state of $\mathbf{I}^{(-)}$*; HOMO that is localized in the deprotonated indole ring is almost orthogonal to LUMO (see Figure 7). The extensive localization of the MOs depending on the two functional moieties (i.e., the indole ring and the maleimide ring) could enhance the ICT character of $\mathbf{I}^{(-)}$* and simultaneously this enhancement stabilizes the potential energy of the S_1 state. On the other hand, the potential energy of the S_0 state at the twisted structure increases by 6956 cm^{-1} (19.9 kcal mol^{-1}) in comparison with that at the equilibrium geometry. Such a significant destabilization in the S_0 state suggests that a high potential barrier exists against the twisting motion, and finally a drastic twisting results in the large Stokes shift. As

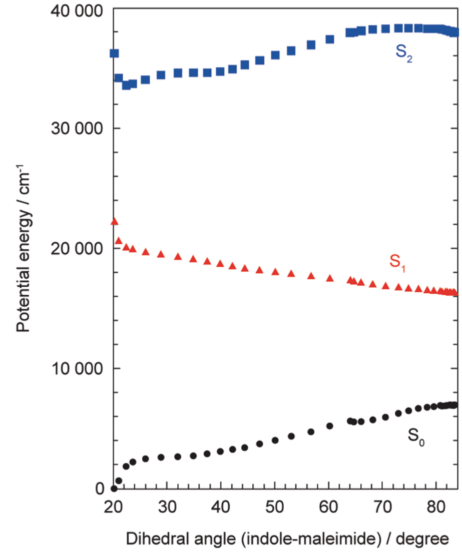

Figure 8. Potential energy curves of the S_0, S_1, and S_2 states against the twisting angle between the indole and the maleimide moieties.

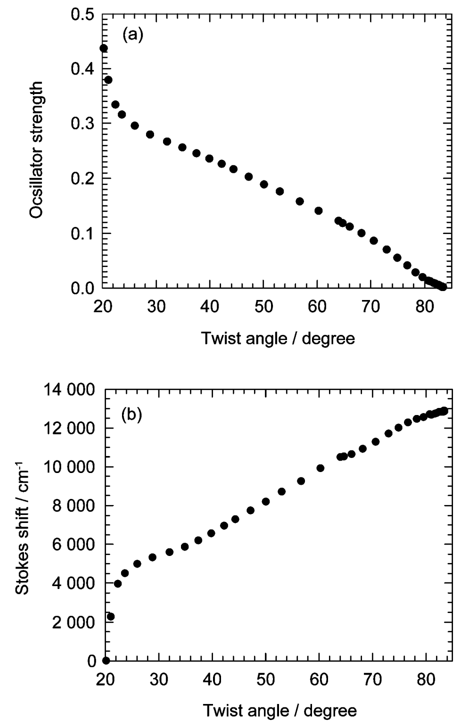

Figure 9. Plots of (a) the oscillator strengths and (b) values of the Stokes shift along the coordinate of the twisting angle between the indole and the maleimide moieties.

seen in Table 3, however, the vertical transition energy between the S_1 and S_0 states at the minimum of S_1 is 9296 cm^{-1}, which corresponds to 1076 nm emission. This wavelength is vastly different from an experimental value (600 nm).[16] The calculated emission frequency is red-shifted by 12 935 cm^{-1} from an absorption (22 231 cm^{-1}) for $\mathbf{I1}^{(-)}$, which means that the theoretically predicted value of Stokes shift is about 2.4 times larger than the experimental value (5457 cm^{-1}).[16] Furthermore, since the calculated oscillator strength (f_0) is 0.002, the S_1-S_0 transition has a forbidden character due to the orthogonality of MOs discussed above. Thus, in anionic **BIM**, the potential minimum would not correspond to the minimum that provides emission. We however found the two minimum energy structures of the S_0 and the S_1 states are quite similar to each other

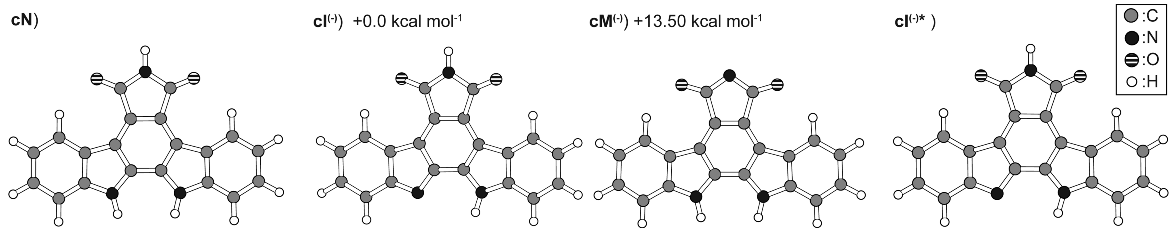

Figure 10. Optimized structures of neutral species (**cN**), the deprotonated anions (**cI**$^{(-)}$ and **cM**$^{(-)}$) in the S_0 state and the anion in the S_1 state (**cI**$^{(-)}$*****) of **C-BIM**.

TABLE 4: Potential Energies of the S_0, S_1, and S_2 States and the Oscillator Strengths and the Excitation Energies for the Electronic Transitions of the Neutral Isomer (cN), the Deprotonated Anions (cI$^{(-)}$, cM$^{(-)}$) of C-BIM[a]

	electronic state	E/cm^{-1}	oscillator strength	λ /nm our theo.	λ /nm exp[b]
cN	S_0	0			
	S_1	33793	0.18	296	
	S_2	37581	0.12	266	
cI$^{(-)}$	S_0	0			
	S_1	23674	0.15	422	400
	S_2	32086	0.37	312	315
cM$^{(-)}$	S_0	0 (4720)			
	S_1	34938 (39660)	0.04	286	
	S_2	43627 (48351)	0.62	229	

[a] **cI**$^{(-)}$ is the deprotonated form of the indole NH group, and **cM**$^{(-)}$ is the deprotonated form of the maleimide NH group. Figures in parentheses in the column of E(energy)/cm^{-1} stand for the relative energy to the S_0 state of the most stable isomer. [b] Reference 16.

except for the coordinates of the twisting angle, which is defined as the angle between the deprotonated indole subunit and the maleimide unit (see structures of **I1**$^{(-)}$ and **I**$^{(-)}$***** in Figure 4 and 6, respectively).

In order to explore the topographical feature of the S_1 potential energy surface, we have carried out the geometry optimization of the S_1 state with fixing the twisting angle at several data. The obtained potential energy curves are shown in Figure 8, as a function of the corresponding dihedral angle. The potential curve of the S_1 state corresponds to the minimum energy path (MEP) toward the potential minimum along the twisting coordinate. The negative slope of the S_1 potential curve from 20.2° (**I1**$^{(-)}$) to 83.4° (**I**$^{(-)}$*****) is seen in this figure. This downhill potential curve of the S_1 state suggests that the photoexcited molecule at the FC region of the S_1-S_0 excitation could easily reach the twisted structure through smooth twisting. It is interesting to note that the value of the calculated Stokes shift increases with increasing the twist angle. In contrast, the magnitude of the oscillator strength of the S_1-S_0 transition decreases with increasing the twist angle (see Figure 9). If the emission is Stokes shifted about $\sim$ 5400 cm^{-1}, which corresponds to the difference between the potential energies of the S_0 and the S_1 state, the excited molecule undergoes the transition with visible light at a dihedral angle of about 30° on the way to the twisting. This electronic transition is allowed since the oscillator strength is about 0.27 as plotted in Figure 9. It is likely that the structure of anionic **BIM** that provides emission changes little along the twist angle in the S_1 state. In other words, "intermediate structure" emits during the deprotonated indole ring is twisting. However, the possibility of the S_1-S_0 transition at the local minimum which corresponds to such an "intermediate structure" is considered to be unlikely, because no intermediate structures have been found on the S_1 potential surface in our geometry optimization procedure to find the energy minimum.

We have also investigated the properties of the excited neutral **BIM** denoted as **N***, by performing the molecular geometry optimization to search the energy minimum in the S_1 state. The structure of **N*** and the minimum potential energies are displayed in Figure 6 and Table 3, respectively. In contrast to anionic **I**$^{(-)}$*****, the potential minimum of the S_1 state of **N*** is only slightly shifted from the equilibrium geometry of **N1** (FC region). The dihedral angle of the two indole units with respect to maleimide unit for **N*** is 17.2°; this value decreased by 15.6° from that of **N1** in the S_0 state (32.8°). The S_1-S_0 vertical excitation energy (24 497 cm^{-1}) at the minimum of the S_1 state is also inconsistent with the experimental data, and a theoretical value of Stokes shift from that of the FC region (30 508 cm^{-1}) is 6012 cm^{-1}.

II. Connected Bisindolylmaleimide (C-BIM)/Arcyriaflavin A. ***i. Identification of Conformer in N,N-Dimethylformamide (DMF) Solution.*** Figure 10 shows the minimum-energy structures of a neutral isomer (**cN**) and monovalent anionic isomers (**cI**$^{(-)}$ and **cM**$^{(-)}$) of arcyriaflavin A (connected bisindolylmaleimide, **C-BIM**) in the S_0 state. Isomer **cI**$^{(-)}$ is the deprotonated form of an indole NH subunit, and isomer **cM**$^{(-)}$ is the deprotonated form of the maleimide NH group. Only one stable conformer has been obtained for each species of **C-BIM** since the indole subunits are not flexible due to the existence of central C−C (2−2′) bond connecting the two indole moieties. The potential energies of the S_0, S_1, and S_2 states and the vertical excitation energies (S_1-S_0, S_2-S_0) for isomer **cN**, **cI**$^{(-)}$, and **cM**$^{(-)}$ are given in Table 4. In contrast to **BIM**, the deprotonated form of an indole NH group (**cI**$^{(-)}$) is more stable by 13.50 kcal mol^{-1} than the deprotonated form of the maleimide NH group (**cM**$^{(-)}$). The potential energies of the S_1 and S_2 states of the monovalent anion **cI**$^{(-)}$ are remarkably lowered, whereas those of the other isomers are quite high. The vertical excitation energies of the S_1-S_0 and the S_2-S_0 transitions of isomer **cI**$^{(-)}$ are in good agreement with the experimental data.[16] In addition, the relationship between the calculated oscillator strengths (f_0) for these electronic transitions is consistent with the intensities of the two absorption bands. These results suggest that the **C-BIM** molecule exists as the **cI**$^{(-)}$ form in DMF solution.

ii. MOs and Electronic Configurations of Isomers. The number of the electrons in **C-BIM** is less than that in **BIM** by two, and the S_0 state of **C-BIM** is composed of several electronic configurations,

(inner occupied orbitals)^{162}(82a″)^2(83a″)^2(84a″)^2(85a″)^0-(86a″)^0

(inner occupied orbitals)^{162}(82a″)^2(83a″)^1(84a″)^2(85a″)^1-(86a″)^0

(inner occupied orbitals)^{162}(82a″)^2(83a″)^2(84a″)^1(85a″)^1-(86a″)^0

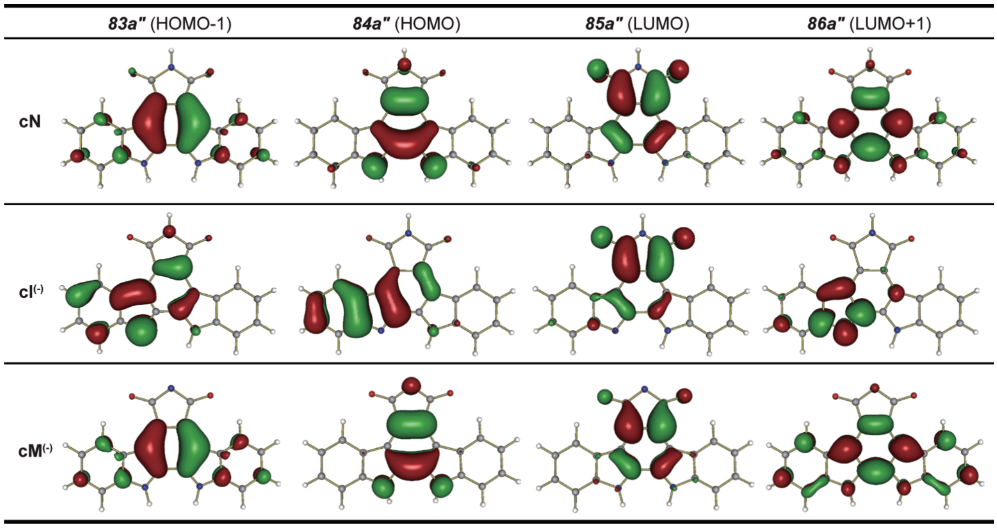

Figure 11. (HOMO-1), HOMO, LUMO, and (LUMO+1) of **cN**, **cI**$^{(-)}$, and **cM**$^{(-)}$.

TABLE 5: Potential Energies of the S_0 and S_1 States and the Oscillator Strengths and the Value of Stokes Shift of the S_0−S_1 Electronic Transition for the Optimized Structure in the S_1 State of the Monovalent Anion of C-BIM (cI$^{(-)}$*)

	electronic state	E/cm^{-1}	oscillator strength	Stokes shift/cm^{-1}
cI$^{(-)}$*	S_0	0		
	S_1	17809	0.07	5866
exp[a]		19802		5276

[a] Reference 16.

(inner occupied orbitals)^{162}(82a″)^2(83a″)^1(84a″)^1(85a″)^0-(86a″)^2

The electronic configurations of the S_0, S_1, and S_2 states are listed in Table S4 of the Supporting Information. The MOs are characterized by 83a″ (HOMO-1), 84a″ (HOMO), 85a″ (LUMO), and 86a″ (LUMO+1) in the C_s symmetry, and we have concerned with five active orbitals which are occupied by six electrons as the active space or CAS(6,5). The CSFs are generated with the following configuration:

[(82a″)(83a″)(84a″)(85a″)(86a″)]^6.

The primary configuration is denoted as (HOMO)^1 → (LUMO)^1 in the deprotonated isomers, **cI**$^{(-)}$ and **cM**$^{(-)}$, whereas that of **cN** is (HOMO-1)^1 → (LUMO)^1. As compared with **BIM**, the ratio of secondary configuration is high (∼25%) in **cN** and **cM**$^{(-)}$ (see also Table S4). Figure 11 illustrates low-energy MOs, (HOMO-1), HOMO, LUMO, and (LUMO+1) of the three isomers. It is notable that the MOs of **cI**$^{(-)}$ tend slightly to the deprotonated indole subunit whereas the MOs of **cN** and **cM**$^{(-)}$ are symmetric with respect to the center of the molecule. As is the case of **BIM**, HOMO−LUMO or (HOMO-1)−(LUMO) excitation of isomer **cI**$^{(-)}$ corresponds to an electron transfer from π-MO localized on the deprotonated indole moiety to π*-MO localized on the maleimide moiety, and these electronic transitions suggest the occurrence of ICT. The ICT character lowers the energies of the excited states. This may be the reason why the S_1−S_0 or S_2−S_0 vertical excitation energies are lower than the other two species.

iii. Optimized Structure of Excited State and Origin of Stokes Shift. Our calculation suggests that most part of the absorption spectrum of **C-BIM** is contributed by the **cI**$^{(-)}$ form and the S_2−S_0 excitation is the primary process of the photoexcitation. In order to examine the potential minimum where the molecule de-excites, we carried out geometry optimization of the molecular structure on the S_1 state potential surface for the monovalent anion which is deprotonated form of an indole NH group. According to the Kasha rule,[23] the molecule excited into the S_2 state from the S_0 state emits fluorescence from the S_1 state in the solution phase. The electronic relaxation from the S_2 state to the S_1 state is considered to be the origin of the Stokes shift of **C-BIM**. The optimized structure in the S_1 state of the anion of **C-BIM** or **cI**$^{(-)}$* is displayed in Figure 10. The potential energy and the vertical transition energy to the S_1 state are given in Table 5. The equilibrium geometry of **cI**$^{(-)}$* is planar, and it also similar to the geometry in the FC region (**cI**$^{(-)}$) the HOMO−LUMO singly excited configuration (88%) is primary configuration of the S_1 state. The vertical transition energy between the S_1 and the S_0 states of **cI**$^{(-)}$* is 17809 cm^{-1}. This energy corresponds to 562 nm emission, providing a theoretical Stokes shift is 5866 cm^{-1}. The experimental values[16] for the emission energy and the Stokes shift are 19 802 cm^{-1} (505 nm) and 5276 cm^{-1}, respectively. These values are in moderate agreement with the theoretical results.

Conclusions

In this paper we discuss the photophysical properties of two fluorescent indole derivatives, **BIM** (or arcyriarubin A) and **C-BIM** (or arcyriaflavin A) on the basis of quantum chemistry calculations. The occurrence of ICT in **BIM** and **C-BIM** is a subject of controversy. Our results have brought an explanation of the issue. The neutral species and the monovalent anion that is deprotonated from the maleimide NH group of **BIM** show no transitions containing the ICT character. The ICT character significantly depends on the shape of molecular orbitals. In these species, the MOs involved in low-energy electronic transitions are symmetric. The monovalent anion which is deprotonated from an indole NH group of **BIM** exhibits that some electron excitations correspond to the ICT. **C-BIM** shows a similar tendency to **BIM**. Single deprotonation from one of the indole NH groups makes the MOs asymmetric, which may be a reason why their photophysical aspects of the anions of **BIM** and **C-BIM** are similar to the asymmetric indolylmaleimides.[30] The transition of electron to an antibonding π*-MO causes destabilization of the molecule, but the ICT interaction stabilizes the excited states. These properties are consistent with solvatochromic trends. Consequently, we conclude that the ICT occurs in **BIM** and **C-BIM** in the aprotic polar solvents as *N*,*N*-dimethylformamide (DMF).

In contradiction to the similarity of properties of the electronic ground state of **BIM** and **C-BIM**, the behavior of **BIM** in the electronic excited states after photoexcitation is quite different from that of **C-BIM**. In **C-BIM**, the S_2-S_1 excitation is the initial process of the photoabsorption. In solution, the molecule in the S_2 state immediately relaxes after photoexcitation to the S_1 state, hence the Stokes-shifted emission arises from the minimum of the S_1 potential energy surface. The potential minimum geometry of **C-BIM** in the S_1 state is planar. In contrast, the potential energy minimum of the S_1 state of **BIM** corresponds to the twisted structure, where the dihedral angle between a maleimide plane and the deprotonated indole ring is 83.4°. But at the minimum, the orthogonality of MOs closely related to the S_1-S_0 transition would make the transition optically forbidden. Our calculations suggest that the structure of **BIM** that provides emission have a minor change of the twist angle in the S_1 state, or the emission could be from the "intermediate structure" when the deprotonated indole ring is twisting. However, such an intermediate structure has not been obtained as the local minimum of the potential energy surface in our geometry optimization procedure. To solve this question, ab initio molecular dynamics (ab initio MD) simulations would be useful.

Acknowledgment. This study was supported by a Grant-in-Aid for Scientific Research (B) (No. 19350013), Scientific Research in Priority Area (461) "Molecular Theory for Real Systems" (No. 19029034) and (477) "Molecular Science for Supra Functional Systems - Development of Advanced Methods for Exploring elementary Processes" (19056005), the Global COE Program, "Science for Future Molecular Systems" from the Japanese Ministry of Education, Sports, Science and Technology (MEXT), Japan, and Research Fellow of the Japan Society for the Promotion of Science (JSPS).

Supporting Information Available: Additional tables of data. This material is available free of charge via the Internet at http://pubs.acs.org.

References and Notes

(1) Steglich, W.; Steffan, B.; Kopanski, L.; Eckhardt, G. *Angew. Chem., Int. Ed. Engl.* **1980**, *19*, 459–460.

(2) (a) Omura, S.; Iwai, Y.; Hirano, A.; Nakagawa, A.; Awaya, J.; Tsuchiya, H.; Takahashi, Y.; Masuma, R. *J. Antibiot.* **1977**, *30*, 275–282. (b) Furusaki, A.; Hashiba, N.; Matsumoto, T.; Hirano, A.; Iwai, Y.; Omura, S. *J. Chem. Soc., Chem. Commun.* **1978**, 800–801.

(3) Bush, J. A.; Long, B. H.; Catino, J. J.; Bradner, W. T. *J. Antibiot.* **1987**, *40*, 668–678.

(4) Eastman, A.; Kohn, E. A.; Brown, M. K.; Rathman, J.; Livingstone, M.; Blank, D. H.; Gribble, G. W. *Mol. Cancer Ther.* **2002**, *1*, 1067–1078.

(5) Makino, M.; Sugimoto, H.; Shiro, Y.; Asamizu, S.; Onaka, H.; Nagano, S. *Proc. Natl. Acad. Sci. U.S.A.* **2007**, *104*, 11591–11596.

(6) Nishizuka, Y. *Nature* **1984**, *308*, 693–698.

(7) Bit, R. A.; Davis, P. D.; Elliott, L. H.; Harris, W.; Hill, C. H.; Keech, E.; Kumar, H.; Lawton, G.; Maw, A.; Nixson, J. S.; Vesey, D. R.; Wadsworth, J.; Wilkinson, S. E. *J. Med. Chem.* **1993**, *36*, 21–29.

(8) Sapsford, K. E.; Berti, L.; Medintz, I. L. *Angew. Chem., Int. Ed.* **2006**, *45*, 4562–4588.

(9) (a) Kricka, L. *J. Anal. Chem.* **1995**, *67*, 499R–502R. (b) Kricka, L. *J. Anal. Chem.* **1999**, *71*, 305R–308R.

(10) Shimomura, O. *Bioluminescence: Chemical Principles And Methods*; World Scientific Publishing Co., Pte., Ltd.: Singapore, 2006.

(11) Sasaki, E.; Kojima, H.; Nishimatsu, H.; Urano, Y.; Kikuchi, K.; Hirata, Y.; Nagano, T. *J. Am. Chem. Soc.* **2005**, *127*, 3684–3685.

(12) Lee, D.; Khaja, S.; Velasquez-Castano, J. C.; Dasari, M.; Sun, C.; Petros, J.; Taylor, W. R.; Murthy, N. *Nat. Mater.* **2007**, *6*, 765–769.

(13) Kogure, T.; Karasawa, S.; Araki, T.; Saito, K.; Kinjo, M.; Miyawaki, A. *Nat. Biotechnol.* **2006**, *24*, 577–581.

(14) Balemans, M. G.; van de Veerdonk, F. C. *Experientia* **1967**, *23*, 906–907.

(15) (a) Philbrook, G. E.; Ayers, J. B.; Garst, J. F.; Totter, J. R. *Photochem. Photobiol.* **1965**, *4*, 869–876. (b) Nakamura, H.; Goto, T. *Photochem. Photobiol.* **1979**, *30*, 27–33.

(16) Nakazono, M.; Nanbu, S.; Uesaki, A.; Kuwano, R.; Kashiwabara, M.; Zaitsu, K. *Org. Lett.* **2007**, *9*, 3583–3586.

(17) Kaletas, B. K.; Mandl, C.; van der Zwan, G.; Fanti, M.; Zerbetto, F.; De Cola, L.; König, B.; Williams, R. M. *J. Phys. Chem. A* **2005**, *109*, 6440–6449.

(18) Chiu, C.-W.; Chow, T. J.; Chuen, C.-H.; Lin, H.-M.; Tao, Y.-T. *Chem. Mater.* **2003**, *15*, 4527–4532.

(19) Grabowski, Z. R.; Rotkiewics, K. *Chem. Rev.* **2003**, *103*, 3899–4031.

(20) Birks, J. B.; Christophorou, L. G. *Spectrochim. Acta* **1963**, *19*, 401–410.

(21) Taylor, C. A.; El-Bayoumi, M. A.; Kasha, M. *Proc. Natl. Acad. Sci. U.S.A.* **1969**, *63*, 253–260.

(22) (a) Maroncelli, M. *J. Mol. Liq.* **1993**, *57*, 1–37. (b) Nagasawa, Y.; Ando, Y.; Kataoka, D.; Matsuda, H.; Miyasaka, H.; Okada, T. *J. Phys. Chem. A* **2002**, *106*, 2024–2035.

(23) Kasha, M. *Discuss. Faraday Soc.* **1950**, *9*, 14–19.

(24) Kamlet, M. J.; Abboud, J.-L. M.; Abraham, M. H.; Taft, R. W. *J. Org. Chem.* **1983**, *48*, 2877–2887.

(25) Kosower, E. M.; de Souza, J. R. *Chem. Phys.* **2006**, *324*, 3–7.

(26) Kaletas, B. K.; Joshi, H. C.; van der Zwan, G.; Fanti, M.; Zerbetto, F.; Goubitz, K.; De Cola, L.; König, B.; Williams, R. M. *J. Phys. Chem. A* **2005**, *109*, 9443–9455.

(27) Werner, H.-J. *Mol. Phys.* **1996**, *89*, 645–661.

(28) Dunning, T. H., Jr. *J. Chem. Phys.* **1993**, *98*, 1358–1371.

(29) (a) Werner, H.-J.; Knowles, P. J. *J. Chem. Phys.* **1985**, *82*, 5053–5063. (b) Knowles, P. J.; Werner, H.-J. *Chem. Phys. Lett.* **1985**, *115*, 259–267.

(30) Werner, H.-J.; Knowles, P. J.; Lindh, R.; Manby, F. R.; Schütz, M.; Celani, P.; Korona, T.; Rauhut, G.; Amos, R. D.; Bernhardsson, A.; Berning, A.; Cooper, D. L.; Deegan, M. J. O.; Dobbyn, A. J.; Eckert, F.; Hampel, C.; Hetzer, G.; Lloyd, A. W.; McNicholas, S. J.; Meyer, W.; Mura, M. E.; Nicklass, A.; Palmieri, P.; Pitzer, R.; Schumann, U.; Stoll, H.; Stone, A. J.; Tarroni, R.; Thorsteinsson, T. MOLPRO, version 2006. 1; a package of ab initio programs (see http://www.molpro.net).

JP9043489